The Radiation Monitoring of the Mangrove Plants in Egypt's Red Sea Coast

Article *in* Egyptian Journal of Aquatic Biology and Fisheries · July 2024

DOI: 10.21608/EJABF.2024.367784

5 authors, including:

Atef El-Taher
Al-Azhar University
274 PUBLICATIONS **4,886** CITATIONS

Egyptian Journal of Aquatic Biology & Fisheries
Zoology Department, Faculty of Science,
Ain Shams University, Cairo, Egypt.
ISSN 1110 –6131
Vol. 28(4): 177–190 (2024)
www.ejabf.journals.ekb.eg

The Radiation Monitoring of the Mangrove Plants in Egypt's Red Sea Coast

Shaimaa M. Magdy[1*], Atef El-Taher[2, 3], Islam M. Nabil[4], Adel G.E. Abbady[5], Hashem Abbas Madkour[1]

[1]National Institute of Oceanography and Fisheries, Alexandria, Egypt
[2]Physics Department, Faculty of Science, Al-Azhar University, Assuit Branch, 71542 Assuit, Egypt
[3]Department of General Educational Development, Faculty of Science and Information Technology, Daffodil International University, Ashulia, Dhaka - 1341, Bangladesh
[4]Physics Department, Faculty of Science, Fayoum University, Fayoum, Egypt
[5]Physics Department, South Valley University, Faculty of Science, Qena, Egypt

Coresponding Author: drshmmelgamal@gmail.com

ARTICLE INFO

Article History:
Received: Jan. 11, 2024
Accepted: May 8, 2024
Online: July 17, 2024

Keywords:
Mangrove plants,
Gamma spectroscopy,
Radiation hazard,
HPGe

ABSTRACT

The assessment of the radioactivity level and associated risks has been performed for the mangrove plants. Twenty-five mangrove samples were collected from the Abu Fasi, Marsa Shaab, and Sowmaa mangroves in the Marsa Shaab area of the Egyptian Red Sea coast. The activity concentration values of the nuclides 226Ra, 232Th, and 40K for samples collected from sediments associated with the mangrove environments were measured. The specific activities in mangrove samples obtained in the Abu Fasi region varied as follows: 15± 0.8 Bq.kg-1 to 42± 2.1 Bq.kg-1 for 226Ra, 10± 0.5 Bq.kg-1 to 39± 1.9 Bq.kg-1 for 232Th, and 103± 5.2 Bq.kg-1 to 340± 17 Bq.kg-1 for 40K. Additionally, the activity concentrations of the mangrove samples collected from Marsa Shaab and Sowmaa mangrove areas ranged as follows: 28± 1.4 to 56± 2.8 Bq.kg-1 for 226Ra, 18± 0.9 to 58± 2.9 Bq.kg-1 for 232Th, and 164± 8.2 to 531± 26.5 Bq.kg-1 for 40K. Moreover, the mangrove samples collected from the Sharm el El Madfea area showed activity concentrations ranging as follows: 25± 1.3 to 52± 2.6 Bq.kg-1, 15± 0.8 to 61± 3 Bq.kg-1, and 250± 9.1 to 583± 29.2 Bq.kg-1 for 226Ra, 232Th, and 40K, respectively. The highest average values were observed in samples collected from Marsa Shaab and Sowmaa mangroves for the 226Ra and 232Th. However, the highest average value for 40K was measured in samples collected from the Sharm El Madfea area. The radiation hazard calculations for the collected mangrove samples showed much lower values than the criterion and worldwide recommended limits.

INTRODUCTION

Numerous wetland habitats along the Egyptian Red Sea coast are of great value to local fauna. Many countries in the tropics and subtropics rely heavily on mangrove resources. The collection of shrubs and trees can tolerate high salt levels in their environment **(Badarudeen *et al.*, 1996)**. Approximately, 525 square kilometers of land in Egypt are covered by mangroves **(Shaltout *et al.*, 2005)**.

Mangrove communities occur in the intertidal zone, growing along brackish and seawater shores and include plants that colonize waterlogged and saline soils. Mangroves also control coastal erosion and contribute to shoreline accretion **(Martin *et al.*, 2019)**. Its growth in the Red Sea has a northern latitudinal limit, which is largely determined by relatively higher air temperatures. Most of the mangrove forests along the Red Sea are too small and thin to be used for lumber or livestock feed **(Elsebaie *et al.*, 2013; Almahasheer *et al.*, 2016)**. Their ecological role includes protecting the coast from erosion and trapping sediments **(Maghrabi, 2009)**.

Mangroves play a crucial role in coastal ecosystems due to their enormous root systems, which protect the coast and provide shelter for marine animals and birds, increasing biodiversity and ensuring the survival of juveniles of economically valuable fish and crustaceans **(A. El-Taher & H. Madkour, 2014; Eid *et al.*, 2016)**. In the mangrove ecosystem and offshore environments, such as among shrimp populations, the presence of mangrove debris like deceased leaves and branches provides a valuable food source **(Qashqari *et al.*, 2020; Palit *et al.*, 2022)**. However, the temperature and salt levels in the area are quite close to the suitable limits for mangrove life, making the mangroves extremely susceptible to disturbance and potentially reducing their capacity for recovery **(Kumar *et al.*, 2010)**.

The southern Red Sea and the Gulf of Aden are home to huge mangrove stands (the Al-Shora plant) **(Madkour, 2015)**. The extensive root systems of mangroves protect the coast from erosion and provide a haven for various marine animals, birds (which increase biodiversity), and juveniles of commercially important fish and crustaceans **(Karimi *et al.*, 2022)**.

Four species of mangrove have been recorded from the Red Sea: *Avicennia marina*, which is found throughout the study area; *Rhizophora mucronata*, which is found at only a few locations in Saudi Arabia, Egypt, Sudan, and Ethiopia (Eretria currently); *Bruguiera gymnorhiza* recorded from Sudan and a single location in north Yemen, and *Ceriops tagal*, recorded from Musseri Island in Ethiopia (Eretria currently) **(Downton, 1982; Roy *et al.*, 2023)**. Two Red Sea mangrove species were found in the Saudi Arabian and the Egyptian Red Sea coastal zones: *Avicennia marina* and *Rhizophora mucronate*. *Avicennia* species are widespread throughout Saudi Arabia and Egypt. At the same time, *Rihizophora mucronate* are located only at six sites in Saudi Arabia and Egypt, and it is begining to appear south of the city of Shalateen.

This study aimed to determine the activity concentrations of ^{226}Ra, ^{232}Th, and ^{40}K radionuclides and radiological hazardous indices related to mangrove plants for selected locations in the southern part of the Egyptian Red Sea coast to monitor the probable releases of environmental radioactivity. Radiation hazard indices, radium equivalent activity (Raeq), internal/external hazard indices (Hin / Hex), and the gamma/alpha index (Iγ, Iα) were calculated and compared against the average worldwide exposure limits.

MATERIALS AND METHODS

1. Samples collections

Twenty-five mangrove samples from the Red Sea coast of Egypt were collected for investigation.Samples 1–9 were collected from the Abu Fasi area, spanning 65km south of Shalaten (35° 55' N, 22° 42' E). Samples 10–17 were collected from the Marsa Shaab and Sowmaa mangrove areas located north of Marsa Shaab and contained the Zigophelluim plant species growing above the beach (22° 50’ N, 35° 45’ E). Samples 18–25 were collected from the Sharm El Madfea area, located south of Shalateen, about 18km (22° 57'N, 35° 40'E). Fig. (1) represents the location of the mangrove-collected sample areas.

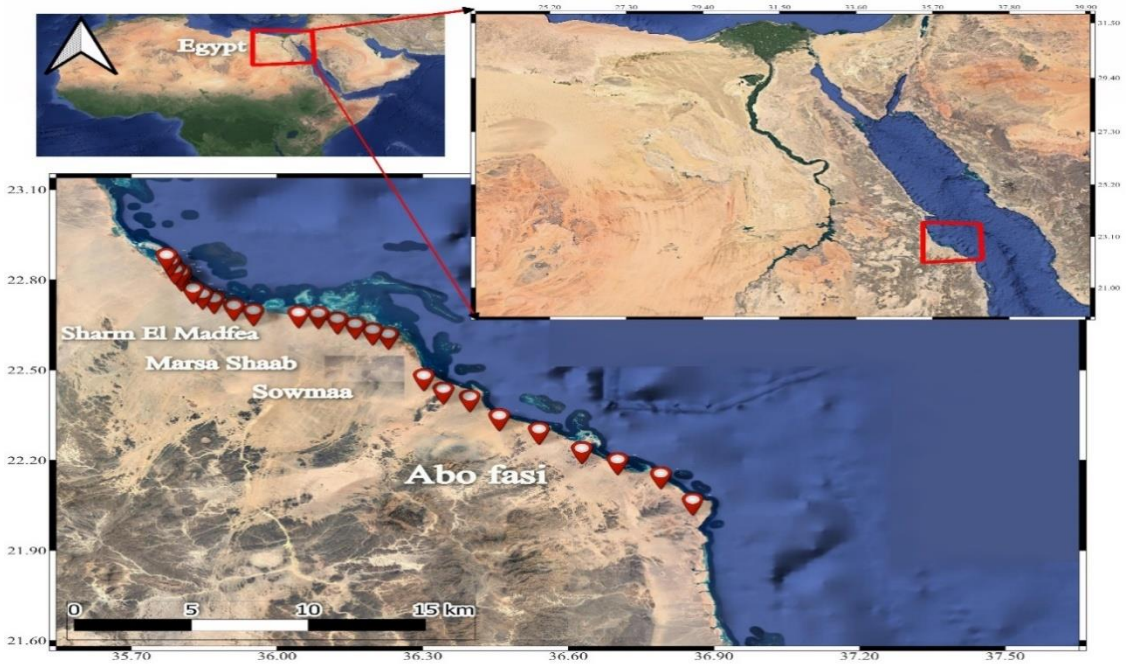

Fig.1. Study areas along the Egyptian Red Sea coast of the collected mangrove samples

2. Samples preparation

Twenty-five samples were collected from sediments associated with the mangrove environment. The samples weighed 1kg. They were dried at 110 degrees Celsius to eliminate any remaining moisture **(Nabil *et al.*, 2024)**. We used a gamma spectrometer to test samples packed in polyethylene bottles of 350cm^3 capacity, each with the same density and geometry as a certified multi-volume standard γ-source. To ensure radioactive equilibrium between ^{222}Rn and its short-lived daughter, the sample containers were hermetically sealed for over a month before the tests **(Nabil *et al.*, 2022)**. This is important for keeping the daughters in the sample and the radon gas within the volume **(Agency, 2004; El-Taher & Madkour, 2011)**.

3. Measurement arrangement

An HPGe detector with a photo peak efficiency of 30% was used for gamma spectroscopic detection. High-voltage electricity, approximately 3kV, runs the HPGe detector. The 1332 KeV γ-transition of ^{60}Co, detector showed a resolution of energy of 1.85 keV. Point sources of ^{60}Co, ^{137}Cs, ^{241}Am, and ^{109}Cd were used to calibrate the γ-spectrometer's energy. The efficiency calibration was performed using a volumetric standard source with the same geometry and density. The detector was protected by a 10cm lead shield that is both high-performance and low-background. Quality control (QC) procedures involved reference samples Cu 2010, 312, and 375 from the International Atomic Energy Agency (IAEA) and the Environmental Monitoring Laboratory (EML), Department of Energy (DOE), USA **(Menezes *et al.*, 2023)**. When using a multichannel analyzer (MCA), the channel numbers that correspond to the centers of each full-energy photo peak (FEP) were calculated sincethe counting of calibration source energy takes 8h and because well-defined photo peaks were produced **(Nabil *et al.*, 2023)**.

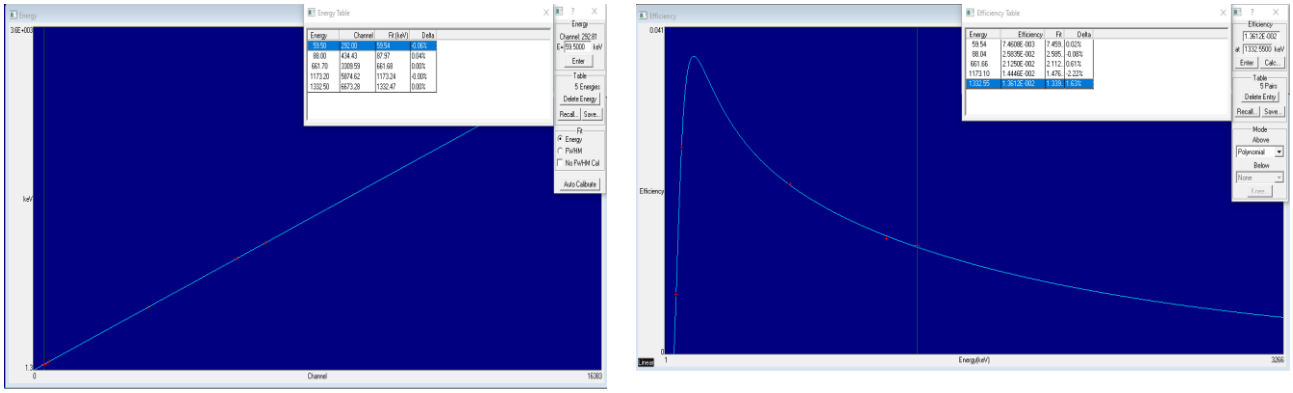

Fig. 2. (a) The energy and (b) the efficiency calibration curves for the used certified standard source

The collected samples' gamma-ray spectra were measured for 24 hours **(Elsayed *et al.* 2021; Sayed *et al.*, 2021)**. The assessment involved subjecting an unoccupied polystyrene container to the same testing procedures and duration as the samples to assess the background distribution owing to radionuclides that are naturally present in the environment near the detector in the laboratory. Specific activity concentrations of the mangrove samples were estimated after background measurements. The schematic of an ultra-sensitive radiometric analysis system using an HPGe detector is shown in Fig. (3).

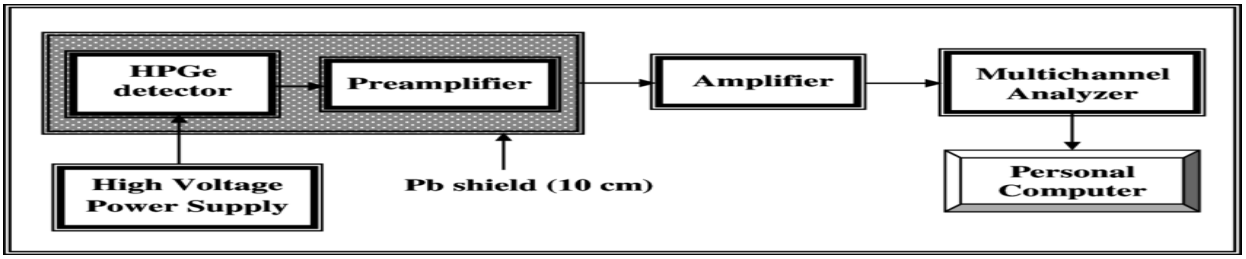

Fig. 3. An ultra-sensitive radiometric analysis system scheme with HPGe detector

4. Gamma spectrometry

The amounts of ^{232}Th, ^{238}U, and their decay products were determined by taking the average of ^{212}Pb, ^{208}Tl, and ^{228}Ac in the samples. For ^{238}U, the amounts were determined by taking the average of ^{214}Pb and ^{214}Bi. This established a secular equilibrium between the nuclides and their decay products **(El-Taher & Madkour, 2011; A. El-Taher & H. A. Madkour, 2014; Ramadan *et al.* 2022)**.

We used the following equation to figure out the activity levels (Ac), in Bq.kg^{-1}, of the γ-transitions coming from the daughter radionuclides of the ^{226}Ra, ^{232}Th decay series, and ^{40}K decay series in the samples that were

$$A_c = \frac{C}{I\gamma \times t \times \varepsilon \times \mathrm{M}} (1)$$

Where, C is the net count at a given energy transition; Iγ is the emission probability of a gamma transition having certain gamma photons per disintegration; t is the counting time; ε photo peak efficiency at a certain energy transition, and M is the mass of the measured sample (kg).

5. Radiation hazard indices calculations

5.1 Radium equivalent (Ra_{eq})

The amounts of ^{226}Ra, ^{232}Th, and ^{40}K in mangroves are generally used to figure out their natural radioactivity. As Ra and its daughter products are responsible for 98.5% of the radioactive effects of the U series; the ^{238}U has been replaced by the decay product ^{226}Ra for its long half-life. The three different indices were used to figure out the γ-ray radiation risks from the radionuclides found in the mangrove samples. This is how to measure radium equivalent activity: it takes into account the radiation risks of ^{226}Ra, ^{232}Th, and ^{40}K activities and add them up **(El-Taher *et al.*, 2010; Nguyen & Trinh 2022; Taalab *et al.*, 2023)**.The radium equivalent (Raeq) was calculated using following the equation:

$$\text{Raeq, Bq.kg}^{-1} = \mathrm{Ac_{Ra}} + 1.43 \times \mathrm{Ac_{Th}} + 0.077 \times \mathrm{Ac_K} \quad (2)$$

For safe utilization, the highest acceptable level of Raeq should not exceed 370.0 Bq/kg. The two different indices represent radiation risks from the outside and inside the body.

5.2 Internal and external hazard index (H_{in}, H_{ex})

To maintain radiation exposure at an insignificant level, the index value should be below one. This ensures that the radiation hazard, specifically the exposure resulting from the radioactivity of the materials, is restricted to 1.0 mSv.y^{-1}. Subsequently, the internal/external hazard index can be articulated as follows:

$$H_{in} = A_cRa/185 + A_cTh/259 + A_cK/4810 \quad (3)$$

$$H_{ex} = A_cRa/370 + A_cTh/259 + A_cK/4810 \quad (4)$$

5.3 Gamma-index (Iγ)

The gamma index (Iγ) encompasses various gamma-ray indices and assessment indicators related to both internal and external radiation emitted by the materials. The threshold for significance

was set at I < 1. The following formula was used to calculate this index **(Attallah *et al.*, 2019; Tamilarasi *et al.*, 2022)**:

$$I\gamma = A_cRa/150 + A_cTh/100 + A_cK/1500 \quad (5)$$

5.4 Alpha index (Iα)

To assess the exposure level due to radon inhalation originating from building materials, alpha indices have been proposed. The critical limit was$I\alpha < 1$. The alpha index was determined,as shown by **Kellerer *et al.*(2001)** and **Valentin (2007**):

$$I\alpha = A_cRa/200 \quad (6)$$

RESULTS AND DISCUSSION

1. The activity concentrations of the collected samples

In Table (1) and Fig. (3a–c), one can see the activities of ^{226}Ra, ^{232}Th, and ^{40}K in mangrove samples from the three locations. For ^{226}Ra, the activity levels of samples 1–9 from the Abu Fasi area ranged as follows: 15± 0.8 $Bq.kg^{-1}$ to 42± 2.1 $Bq.kg^{-1}$, for ^{232}Th, 10± 0.5 $Bq.kg^{-1}$ to 39± 1.9 $Bq.kg^{-1}$, and for ^{40}K, 103± 5.2 $Bq.kg^{-1}$to 340± 17 $Bq.kg^{-1}$. Moreover, the activity levels of the 10–17 mangrove samples from Marsa Shaab and Sowmaa ranged as follows:28± 1.4 $Bq.kg^{-1}$ to 56 ± 2.8 $Bq.kg^{-1}$ for ^{226}Ra, 18± 0.9 $Bq.kg^{-1}$to 58± 2.9 $Bq.kg^{-1}$for ^{232}Th, and 164± 8.2 $Bq.kg^{-1}$to 531± 26.5 Bq.kg-1 for ^{40}K. Also, the mangrove samples (18–25) from the Sharm el Madfea area had activity levels ranging as follows:25± 1.3 $Bq.kg^{-1}$ to 52± 2.6 $Bq.kg^{-1}$ for ^{226}Ra, 15± 0.8 $Bq.kg^{-1}$ to 61± 3 $Bq.kg^{-1}$ for ^{232}Th, and 250± 9.1 $Bq.kg^{-1}$ to 583± 29.2 $Bq.kg^{-1}$ for ^{40}K. The highest average values were observed in samples collected from Marsa Shaab and Sowmaa mangroves for the ^{226}Ra and ^{232}Th. However, the highest average value was observed in samples collected from the Sharm El Madfea area for ^{40}K. According to these results of the activity concentrations, the mangrove samples have a lower activity concentration of the radionuclides ^{226}Ra, ^{232}Th, and ^{40}K, which indicates that they are safe from the point of radiation protection. Table (2**)** lists the activity concentrations of ^{226}Ra, ^{232}Th, and ^{40}K for the mangrove samples of this study compared with those of published studies.

Table 1. Activity concentrations of ^{226}Ra, ^{232}Th, and ^{40}K in the mangrove samples

Sample ID	Location	Activity concentrations ($Bq.kg^{-1}$)		
		^{226}Ra	^{232}Th	^{40}K
AF 1	Abu Fasi	35 ± 1.5	19 ±1.0	215 ±10.1
AF 2		28 ± 2.0	10 ±0.5	165 ±8.2
AF 3		33 ± 1.7	22 ±1.1	206 ±10.3
AF 4		27 ± 1.3	22 ±1.1	103 ±5.2
AF 5		15 ± 0.8	20 ±1.0	195 ±9.8
AF 6		27 ± 1.4	34 ±1.7	299 ±14.9
AF 7		42 ± 2.1	39 ±1.9	340 ±17.0
AF 8		23 ± 1.5	19 ±1.0	215 ±10.1
AF 9		35 ± 1.8	30 ±1.5	221 ±11.1
Average		29.4 ± 1.5	23.8 ± 1.2	217.6 ± 10.7
MS 10	Marsa Shaab and Sowmaa	43 ± 2.1	26 ±1.3	531 ±26.5
MS 11		53 ± 2.7	53 ±2.6	415 ±20.8
MS 12		39 ± 2.0	36 ±1.8	351 ±17.6
MS 13		33 ± 1.6	37 ±1.9	164 ±8.2
MS 14		40 ± 2.0	45 ±2.3	366 ±18.3
MS 15		56 ± 2.8	58 ±2.9	250 ±9.1
MS 16		28 ± 1.4	18 ±0.9	306 ±15.3
MS 17		32 ±1.5	19 ±1.0	215 ±10.1
Average		40.5 ± 2	36.5 ± 1.8	324.7 ± 15.7
SM 18	Sharm El Madfea	34 ± 1.7	41 ±2.0	231 ±11.5
SM 19		30 ± 1.5	16 ±0.8	250 ±9.1
SM 20		34 ± 1.7	14 ±0.7	517 ±25.9
SM 21		35 ± 1.8	15 ±0.8	446 ±22.3
SM 22		25 ± 1.3	14 ±0.7	266 ±26.3
SM 23		52 ± 2.6	61 ±3.0	583 ±29.2
SM 24		40 ± 2.0	21 ±1.0	525 ±26.2
SM 25		47 ± 2.4	45 ±2.3	329 ±16.5
Average		37.1 ± 1.8	28.3 ± 1.4	393.3 ± 20.8

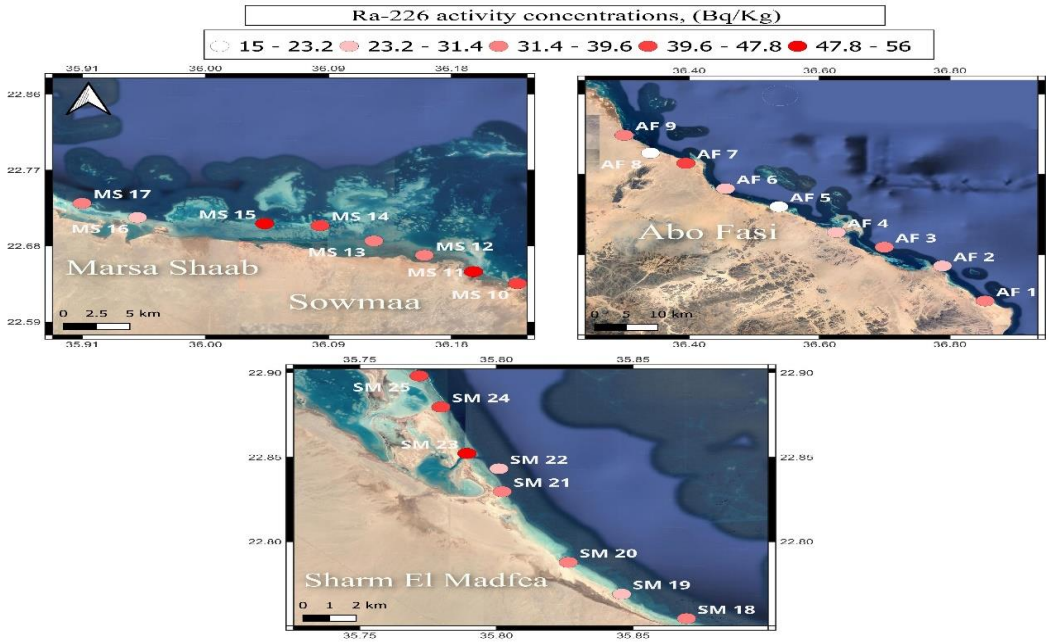

Fig. 3a. Activity concentrations ^{226}Ra for the mangrove samples and their areas

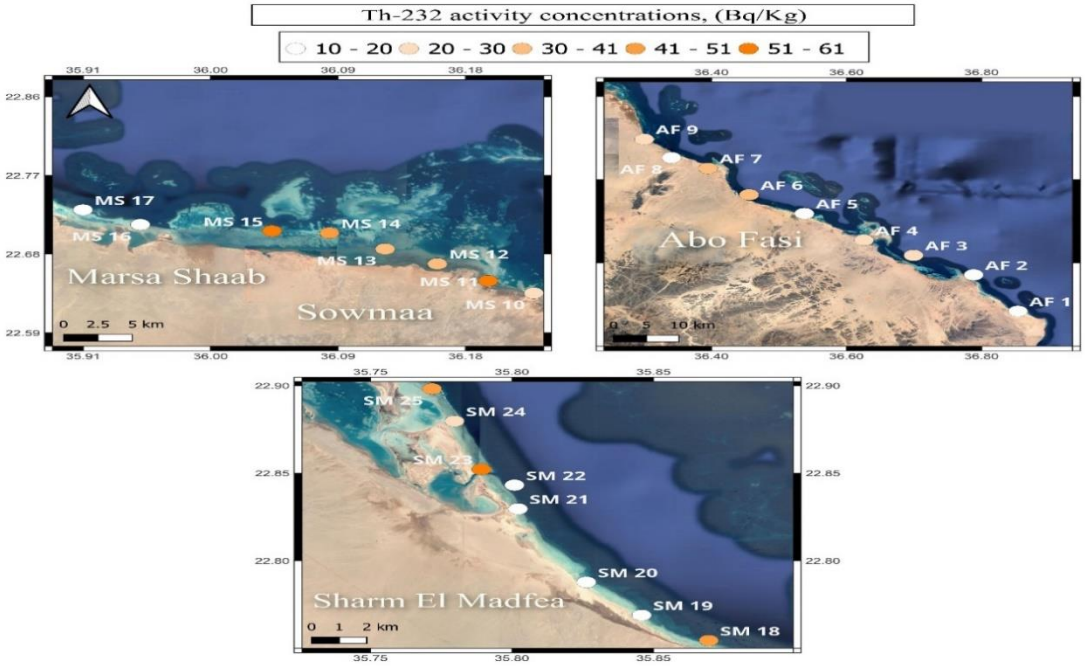

Fig. 3b. Activity concentrations of ^{232}Thin the mangrove samples and their areas

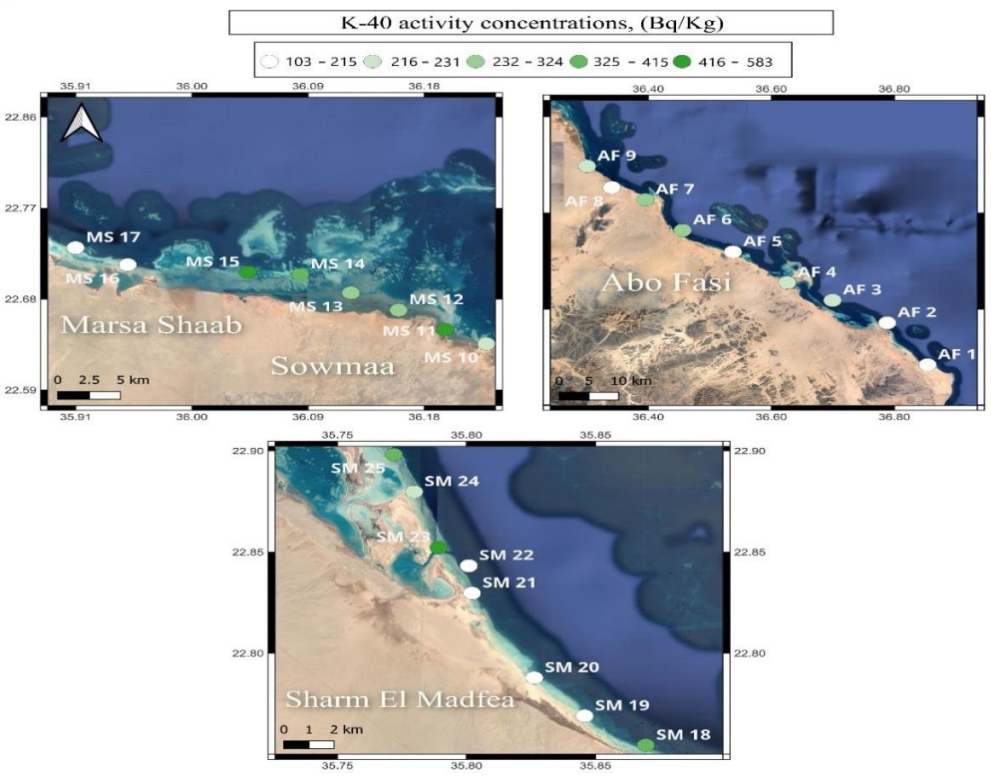

Fig. 3c. Activity concentrations of ^{40}K for the mangrove samples and their areas

Table 2. Comparison between the average activity concentrations of 226Ra, 232Th, and 40K of the mangrove samples in the present study and other published work

Region	Country	Activity concentrations (Bq.kg^{-1})			Reference
		^{226}Ra	^{232}Th	^{40}K	
Abu Fasi	Egypt	**29.4**	**23.8**	**217.6**	**This study**
Marsa Shaab and Sowmaa mangrove		**40.5**	**36.5**	**324.7**	
Sharm El Madfea		**37.1**	**28.3**	**393.3**	
Safaga coast		14.3	17.1	346.5	**(Uosif *et al.*, ٢٠١٦)**
Wadi El-Hamra		18.5	31.1	380.0	**(El-Taher & Madkour, ٢٠١١)**
Wadi El-Esh		20.4	36.3	357.0	
Wadi Abu-Shaar		24.2	35.6	418.0	
Wadi El-Gemal		38.8	47.5	526.0	
Wadi Hamata		35.1	42.5	491.0	
Southeast coast (Pretsunami)	India	25.9	65.1	-	**(Satheeshkumar *et al.*,٢٠١١)**
Southeast coast (Poststunami)		12.2	11.7	-	
Rio Formoso	Brazil	24	41	-	**(Satheeshkumar *et al.*,٢٠١١)**
Chico Science		21	43	-	
Sundarban	Bangladesh	23	16	-	**(Satheeshkumar *et al.*,٢٠١١)**
Pattani Bay	Thailand	4.9	55.8	183.2	**(Satheeshkumar *et al.*,٢٠١١)**
Worldwide		32.0	45.0	412.0	**(Satheeshkumar *et al.*,٢٠١١)**

2. Radiation hazards calculations

Radiation hazards due to specified radionuclides such as ^{226}Ra, ^{232}Th, and ^{40}K were calculated and evaluated to conclude whether an exposed environment or person is safe or not. The values of radiation hazard indices, radium equivalent activity (Ra_{eq}), internal/external hazard indices (H_{in}, H_{ex}), and the gamma/alpha index (Iγ, Iα) were calculated. Radiation risk calculations are based on the amounts of ^{226}Ra, ^{232}Th, and ^{40}K activities found in the samples, as listed in Table (1). Fig.(4) and Table (3) show the radiation hazard calculations for the collected mangrove samples. The radioactivity levels of the mangrove samples varied as follows:55.0 $Bq.kg^{-1}$ to 184.1 $Bq.kg^{-1}$ for Ra_{eq}, 0.1 to 0.5 for H_{ex}, 0.2 to 0.6 for H_{in}, 0.2 to 0.7 for Iγ, and 0.1 to 0.3 for Iα. These results show much lower values than the criteria and worldwide recommended limits.

Table 3. Results of radiation hazard calculations for the mangrove samples

Sample ID	Radiation hazard indices				
	Ra_{eq} ($Bq.kg^{-1}$)	H_{ex}	H_{in}	Iγ	Iα
AF 1	78.7	0.2	0.3	0.3	0.2
AF 2	55.0	0.1	0.2	0.2	0.1
AF 3	80.3	0.2	0.3	0.3	0.2
AF 4	66.4	0.2	0.3	0.2	0.1
AF 5	58.6	0.2	0.2	0.2	0.1
AF 6	98.6	0.3	0.3	0.4	0.1
AF 7	124.0	0.3	0.4	0.4	0.2
AF 8	66.7	0.2	0.2	0.2	0.1
AF 9	94.9	0.3	0.4	0.3	0.2
MS 10	121.1	0.3	0.4	0.5	0.2
MS 11	160.7	0.4	0.6	0.6	0.3
MS 12	117.5	0.3	0.4	0.4	0.2
MS 13	98.5	0.3	0.4	0.3	0.2
MS 14	132.5	0.4	0.5	0.5	0.2
MS 15	158.2	0.4	0.6	0.6	0.3
MS 16	77.3	0.2	0.3	0.3	0.1
MS 17	75.7	0.2	0.3	0.3	0.2
SM 18	110.4	0.3	0.4	0.4	0.2
SM 19	72.1	0.2	0.3	0.3	0.2
SM 20	93.8	0.3	0.3	0.4	0.2
SM 21	90.8	0.2	0.3	0.3	0.2
SM 22	65.5	0.2	0.2	0.2	0.1
SM 23	184.1	0.5	0.6	0.7	0.3
SM 24	110.5	0.3	0.4	0.4	0.2
SM 25	136.7	0.4	0.5	0.5	0.2
Maximum	184.1	0.5	0.6	0.7	0.3
Unscair 2000	370	1	1	1	1

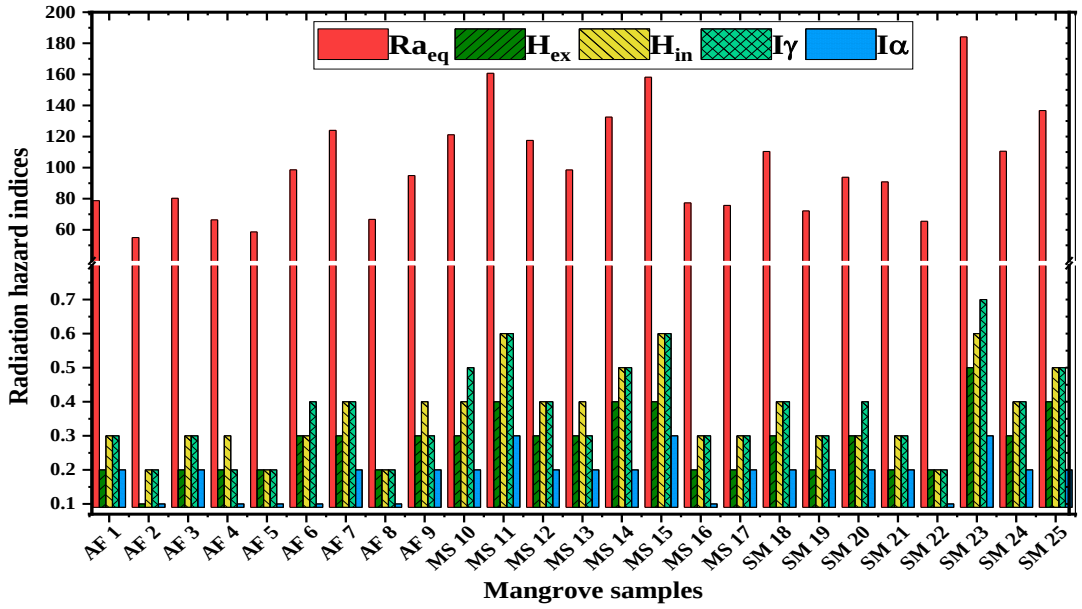

Fig. 4. Radiation hazard indices of the collected mangrove samples

CONCLUSION

This study was conducted to assess the radiological characteristics of mangroves using a gamma ray spectrometer of 25 samples and calculation of the radiological hazard index. The results showed that the mangrove collected from Abu Fasi and Sharm El Madfea contained lower activity concentration values for ^{226}Ra and^{232}Th than samples collected from Marsa Shaab, Sowmaa Marsa. The radiation hazard calculations for the collected mangrove samples showed much lower values than the criterion and worldwide recommended limits. The radiation hazard calculations, including radium equivalent activity (Ra_{eq}), internal and external hazard indices (H_{in} and H_{ex}), and the gamma and alpha indices (Iγ and Iα), for the collected mangrove samples were much lower than the criteria and worldwide recommended limits deemed safe for any industrial applications.

REFERENCES

Agency, I. A. E. (2004). Extent of environmental contamination by naturally occurring radioactive material (NORM) and technological options for mitigation. International Atomic Energy Agency .

Almahasheer, H.;Aljowair, A.; Duarte, C. M.andIrigoien, X .(2016). (Decadal stability of Red Sea mangroves. Estuarine, Coastal and Shelf Science, 169 **:**164-172 .

Attallah, M.; Metwally, S.; Moussa, S. and Soliman, M. A. (2019). Environmental impact assessment of phosphate fertilizers and phosphogypsum waste: elemental and radiological effects. Microchemical Journal, 146: 789-797 .

Badarudeen, A.; Damodaran, K.; Sajan, K. and Padmalal, D. (1996). Texture and geochemistry of the sediments of a tropical mangrove ecosystem, southwest coast of India. Environmental Geology, 27: 164-169 .

Downton, W. (1982). Growth and osmotic relations of the mangrove Avicennia marina, as influenced by salinity. Functional Plant Biology, **9**(5): 519-528 .

Eid, E. M.; El-Bebany, A. F. and Alrumman, S. A. (2016). Distribution of soil organic carbon in the mangrove forests along the southern Saudi Arabian Red Sea coast. Rendiconti Lincei, 27: 629-637 .

El-Taher, A. and Madkour, H. (2011). Distribution and environmental impacts of metals and natural radionuclides in marine sediments in-frontof different wadies mouth along the Egyptian Red Sea Coast. Applied Radiation and Isotopes, **69**(2): 550-558 .

El-Taher, A. and Madkour, H. (2014). Environmental studies and radio-ecological impacts of Anthropogenic areas: shallow marine sediments Red Sea ,Egypt. J Isot Environ Health Stud, 50: 120-133 .

El-Taher, A. and Madkour, H. A. (2014). Environmental and radio-ecological studies on shallow marine sediments from harbour areas along the Red Sea coast of Egypt for identification of anthropogenic impacts .Isotopes in environmental and health studies, **50**(1): 120-133 .

El-Taher, A.; Makhluf, S.; Nossair, A. and Halim, A. A. (2010). Assessment of natural radioactivity levels and radiation hazards due to cement industry. Applied Radiation and Isotopes, **68**(1): 169-174

Elsayed, A.; Hussein, M.; El-Mongy, S.; Ibrahim, H.; Shazly, A. and Abdel-Rahman, M. (2021). Signature Verification of 235 U/238 U Activity Ratio for Ores and Natural Samples Using γ-Ray Spectrometry and a Derived Equation. Radiochemistry, 63 ,:٦٢٧-٦٣٤.

Elsebaie, I. H.; Aguib, A. S. and Al Garni, D. (2013). The role of remote sensing and GIS for locating suitable mangrove plantation sites along the southern Saudi Arabian Red Sea coast .

Karimi, Z.; Abdi, E.; Deljouei, A.; Cislaghi, A.; Shirvany, A.; Schwarz, M. and Hales, T. C. (2022). Vegetation-induced soil stabilization in coastal area: An example from a natural mangrove forest. Catena, 216: 106410 .

Kellerer, A. M.; Nekolla, E. A. and Walsh, L. (2001). On the conversion of solid cancer excess relative risk into lifetime attributable risk. Radiation and Environmental Biophysics, 40: 249-257 .

Kumar, A.; Khan, M. A. and Muqtadir, A. (2010). Distribution of mangroves along the Red Sea coast of the Arabian Peninsula: Part-I: The northern coastof western Saudi Arabia. Earth Science India, 3 .

Madkour, H. (2015). Detection of damaged areas due to tourism development along the Egyptian Red Sea coast using GIS, remote sensing and foraminifera. State of the Art, National Institute of Oceanographyand Fisheries, Red Sea Branch .

Maghrabi, A. (2009). Parameterization of a simple model to estimate monthly global solar radiation based on meteorological variables, and evaluation of existing solar radiation models for Tabouk, Saudi Arabia. Energy conversion and management, **50**(11): 2754-2760 .

Martin, C.; Almahasheer, H. and Duarte, C. M. (2019). Mangrove forests as traps for marine litter. Environmental Pollution, 247: 499-508 .

Menezes, M. A. d. B. C.; Sabino, C. d. V. S. and Jaćimović, R. (2023). k-‧ Neutron Activation Analysis at CDTN, Brazil: 27 years of history, development and main achievements. Journal of Radioanalytical and Nuclear Chemistry, 1-12 .

Nabil, I. M.; El-Kourghly, K. M. and El Sayed, A. F. (2023) A semi–empirical method for efficiency calibration of an HPGe detector against different sample densities. Applied Radiation and Isotopes, 200, 110946.

Nabil, I. M.; El-Samrah, M. G.; Sayed, A. F. E.; Shazly, A. andOmar, A. (2024). Radionuclides distribution and radiation hazards assessment of black sand separation plant's minerals: a case study. Sci Rep, **14**(1): 5241.

Nguyen, V.-D. and Trinh, D.H. (2022). Natural radioactivity and radiological hazard evaluation in surface soils at the residential area within Ban Gie monazite placer, Nghe An. Journal of Radioanalytical and Nuclear Chemistry, **331**(2): 769-781 .

Palit, K.; Rath, S.; Chatterjee, S. and Das, S. (2022). Microbial diversity and ecological interactions of microorganisms in the mangrove ecosystem: Threats, vulnerability, and adaptations. Environmental Science and Pollution Research, **29**(22): 32467-32512 .

Qashqari, M. S.; Garcias-Bonet, N.; Fusi, M.; Booth, J. M.; Daffonchio, D. and Duarte, C. M. (2020). High temperature and crab density reduce atmospheric nitrogen fixation in Red Sea mangrove sediments. Estuarine, Coastal and Shelf Science, 232: 106487 .

Ramadan, R. S.; Dawood, Y. H.; Yehia, M. M. and Gad, A. (2022). Environmental and health impact of current uranium mining activities in southwestern Sinai, Egypt. Environmental Earth Sciences, **81**(7): 213 .

Roy, U. K.; Sarkar, C.; Jamaddar, S.; Mondal, B.; Ramproshad, S.; Zulfiquar, T. N.; Panthi, S.; Mondal, M.; Mukerjee, N. and Rahman, M. H. (2023). A detailed assessment of the traditional applications, bioactive content,

pharmacology, and toxicity of Rhizophora mucronata. Journal of Herbal Medicine, 100702 .

Satheeshkumar, G.; Hameed, P. S.; Meeramaideen, M. and Kannan, V. (2011). A post-tsunami study on the distribution and bioaccumulation of natural radionuclides in Pichavaram mangrove environment (South East Coast of India) and dose to local human population. Radiation Protection and Environment, **34**(2): 96.

Sayed, M.; El-Mongy, S.; Tawfic, A. and Abdel-Rahman, M. (2021). Validation of the Optimized Parameters for Improvement of Gamma Spectrometers Performance and Efficacy. Physics of Particles and Nuclei Letters, **18**(2): 222-231 .

Shaltout, K.; Khalaf-Allah, A. and El-Bana, M. (2005). Environmental characteristics of the mangrove sites along the Egyptian Red Sea coast. Assessment and management of mangrove forests in Egypt for sustainable utilization and development: a project funded by ITTO (Japan)and supervised by MALR/MSEA—EEAA, Cairo .

Taalab, S. A.; Al Meshari, M.; Alzamil, Y.; Abanomy, A.; Alyahyawi, A. R.; Mohamed, W. H. and El-Taher, A. (2023). Radiological and ecological hazards evaluation of episyenite used as building materials. Journalof Radioanalytical and Nuclear Chemistry, 1-19 .

Tamilarasi, A.; Sathish, V. and Chandrasekaran, A. (2022). Assessment of gamma dose and annual effective dose rate for commonly used fertilizer samples in agriculture field with a statistical approach. Radiation protection dosimetry .

Uosif, M.; Issa, S.; Zakaly, H. M.; Hashim, M. and Tamam, M. (2016). The status of natural radioactivity and heavy metals pollution on marine sediments Red Sea coast, at Safaga, Egypt. Journal of Nuclear Physics, Material Sciences, Radiation and Applications, **3**(2): 191-222 .

Valentin, J. (2007). The recommendations of the international commission on radiological protection **(37).** Elsevier Oxford.